Stress Corrosion Cracking of a Superplastic and Nonsuperplastic Zn-22.3Al Alloy in 3% NaCl Solution

M.S. Yeh, J.C. Chang, and T.H. Chuang

(Submitted 6 April 1998; in revised form 7 November 1998)

Through appropriate heat treatments, a Zn-22.3wt%Al (Zn-22.3Al) alloy can be prepared in both superplastic and nonsuperplastic specimens. It has been found that the superplastic Zn-22.3Al alloy possesses a very fine microduplex structure, while the nonsuperplastic alloy has a lamellar duplex structure with locally coarsened second phases. The very different microstructures of both specimens result in different corrosion and stress corrosion cracking (SCC) behaviors in 3% NaCl solution. In addition, the fractographs of both the superplastic and nonsuperplastic Zn-22.3Al specimens after SCC tests under various anodic applied potentials have been compared. Through the observations, a mechanism for the SCC in this case was proposed to show that the cracks proceeded with successive processes of oxide film rupture and Zn-Al matrix tearing. Such a mechanism is more evident for the fractography of nonsuperplastic specimens, on which a series of parallel strips inserted with dimple-bands can be obviously found.

Keywords duplex structure, nonsuperplastic, stress corrosion cracking (SCC), superplastic, Zn-Al alloy

1. Introduction

Zn-Al is one of the oldest superplastic alloys. In fact, the first use of the word superplasticity in English is believed to have originated in an article by Bochvar and Sviderskaya entitled "Superplasticity in Zn-Al Alloys" (Ref 1). Since then, a number of works dealing with superplastic behavior and other material characteristics of this alloy have been reported (Ref 2-7). Furthermore, the feasibility of producing such an alloy with powder metallurgy has also been reported (Ref 8). For practical applications, it was reported that the British Leyland Motor Corporation and the Rio Tino Zinc Company had developed a superplastic Zn-Al alloy, which could be formed into panels for automobile bodies using conventional techniques for shaping plastics (Ref 9). Another recent example is a Zn-5Al-0.3Mg grooved drum used in the textile industry, which had the attractive advantage of low manufacturing costs (Ref 10).

For the attainment of superplasticity, a eutectoid Zn-22Al alloy was quenched from a temperature above the monotectic temperature (277 °C) to room temperature or lower. The spinodal decomposition of zinc-rich solid solution accompanying this treatment resulted in a fine grain microstructure, which contained an aluminum matrix dispersed by a zinc second phase (Ref 9). After testing at a temperature of 200 to 250 °C with a strain rate of 0.1%/min to 10%/min, the material presented excellent superplastic behavior with a strain rate sensitivity (m value) of 0.4 to 0.66 and an elongation of 500 to 2900% (Ref 11). However, with the annealing treatment of this alloy, which followed the quenching process, a lamellar structure of zinc-rich properties formed in the solid-solution temperatures. In this case, superplasticity did not occur in this alloy (Ref 9). It was interesting to note that due to such a minute difference in heat treatment processes, a Zn-22Al alloy can be produced in superplastic or nonsuperplastic form.

Corrosion damage has been acknowledged as a common problem in the engineering use of Zn-Al alloy, even though the alloy exhibits advantageous superplastic behavior. In the above example of the grooved drum application, the superplastically formed workpieces were plated with a 20 to 25 μm thick Ni-P film for the purpose of corrosion prevention (Ref 10). However, a quantitative evaluation of corrosion properties for such superplastic Zn-Al alloy was scanty. Furthermore, since the superplastic and nonsuperplastic Zn-Al alloys possess quite different microstructures, their corrosion behaviors should also be dissimilar. In a 7475 Al-Zn-Mg alloy, it has been found that a superplastic material exhibits higher stress corrosion cracking (SCC) susceptibility than a nonsuperplastic material, both in a NaCl aqueous solution and in an atmospheric environment (Ref 12).

The discrepancy in stress corrosion behavior was attributed to the different grain boundary precipitate structures and grain sizes between superplastic and nonsuperplastic 7475 Al-Zn-Mg alloys (Ref 12, 13). For the same reason, the stress corrosion behaviors of superplastic and nonsuperplastic Zn-Al alloys are of interest. In this study, a eutectoid Zn-22.3wt%Al alloy was heat treated to obtain superplastic and nonsuperplastic specimens. Their corrosion behaviors were compared through the results of the electrochemical measurements. Furthermore, the stress corrosion fractures of both materials were investigated by constant load testing under electrochemical potential control.

2. Experimental

The Zn-22.3wt%Al alloy (Zn-22.3Al) used in this study was prepared by melting under an argon atmosphere and then cast-

M.S. Yeh, Department of Mechanical Engineering, Chung-Hua University, Hsinchu 300, Taiwan, R.O.C.; **J.C. Chang** and **T.H. Chuang,** Institute of Materials Science and Engineering, National Taiwan University, Taipei, 106 Taiwan, R.O.C.

ing into iron molds. These ingots were homogenized at 623 K for 10 days and then rolled into a 1 mm thick sheet. Experimental specimens were cut from the sheet material. Dimensions of stress corrosion testing specimens are shown in Fig. 1. All specimens were solution treated by heating at 623 K for 4 h, followed by quenching in water. Some of these quenched specimens remained at room temperature and immediately decomposed into a microduplex structure as shown in Fig. 2(a), resulting in superplasticity in this alloy. The other solution-treated specimens were further annealed at 483 K for 48 h and quenched in water, transforming their structures into a nonsuperplastic lamellar structure as shown in Fig. 2(b). It was also found that in certain local positions the lamellar second phases coarsened.

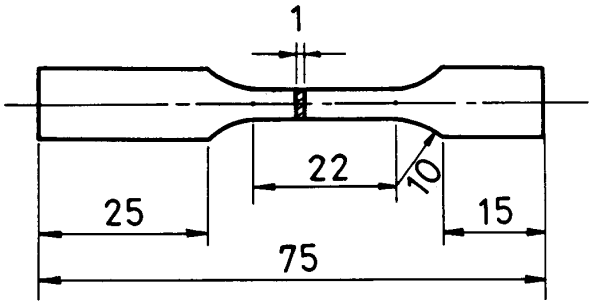

Fig. 1 Dimensions of specimens for stress corrosion cracking tests in millimeters

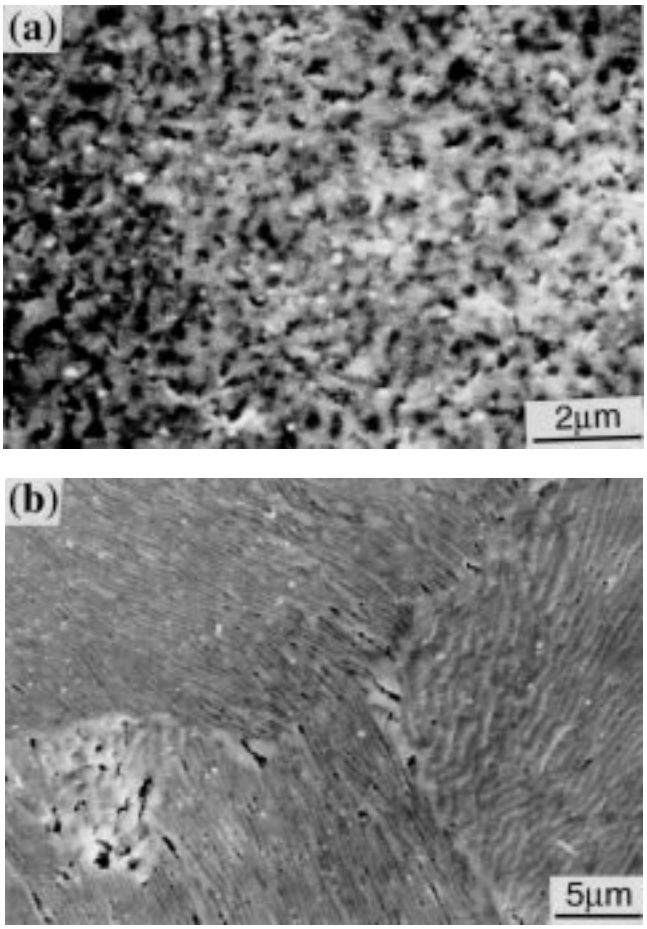

Fig. 2 Microstructure of Zn-22.3Al alloy. (a) Superplastic specimen. (b) Nonsuperplastic specimen

The corrosion behaviors of both specimens were evaluated in 3% NaCl solution using electrochemical techniques. Before the tests, the specimens were ground and polished to 1000 grit SiC paper and degreased in an acetone bath. The open circuit potential, (ϕ_{corr}), was measured versus a saturated calomel electrode (SCE) with an electrometer. For dynamic polarization tests, an EG & G M273A potentiostat (EG & G, Princeton Applied Research, Princeton, NJ) was employed. The potential was scanned from –2.0 V_{SCE} to an anodic current density of 10^4 $\mu A/cm^2$ with a scanning rate of 1 mV/s. The SCC sensitivity in 3% NaCl solution was studied using constant load equipment, and the potential was controlled with a potentiostat. For this purpose, various stress levels were first applied to one set of the SCC specimens, and the failure times of the specimens were recorded at open circuit potential. Then, the failure time for another set of specimens with a fixed stress was measured at various applied potentials. The fracture surfaces after SCC testing were observed using a scanning electron microscope (SEM).

3. Results and Discussion

Before the corrosion studies, both specimens of Zn-22.3Al alloy were subjected to tensile tests in air at room temperature under a strain rate of 10^{-3}/s. Results are shown in Table 1. It can be seen that the nonsuperplastic specimen possessed higher strength but lower elongation. In fact, from the observations of fractured specimens in Fig. 3, it is obvious that the superplastic specimen revealed slight superplasticity even at room temperature under the high strain rate of the tensile tests. The fractographs of both specimens showed a dimple fracture mode (Fig. 4).

The variation of corrosion potential (ϕ_{corr}) with time for both specimens is given in Fig. 5. Long-term stable corrosion potential measurements in 3% NaCl solution are shown in Table 1. Figure 6 shows the dynamic polarization curves for both

Fig. 3 Specimens before and after tensile test at room temperature in air

specimens in 3% NaCl solution. Corrosion data obtained from the polarization curves are also shown in Table 1. The data indicate that the dynamic corrosion potential (ϕ'_{corr}) of superplastic specimens was more active than that of the nonsuperplastic specimens. To evaluate pitting corrosion resistance and the passivation tendency of both specimens, the differences between breakdown potential (ϕ_b) and dynamic corrosion potential were calculated as $\Delta\phi = \phi_b - \phi'_{corr}$. Such a potential difference ($\Delta\phi$) corresponds to the passive range on the polarization curves. From Fig. 5 and Table 1, it is evident that the pitting resistance of both alloys should be similar because both alloys have a similar breakdown potential. However, the superplastic specimen had a wider passive range (larger $\Delta\phi$) than did the nonsuperplastic specimen. The large difference in $\Delta\phi$ for the superplastic alloy is due to its better tendency to passivate.

The higher passivation tendency of this superplastic Zn-22.3Al alloy might be attributed to the more uniform distribution of very fine second-phase particles after spinodal decomposition of this alloy. In the nonsuperplastic Zn-22.3Al alloy, the second phases appeared as a lamellar structure. From Fig 4(b), it can also be observed that at some locations the fine lamellar second phases further decomposed into a coarsened lamellar structure. The less uniform distribution of second phases in the nonsuperplastic specimen might be due to a higher tendency for the local destruction of passive film. In this case, it is reasonable that the passivation tendency of the nonsuperplastic Zn-22.3Al alloy was lower than that of the superplastic alloy. In addition, from Table 1, it was also found that the

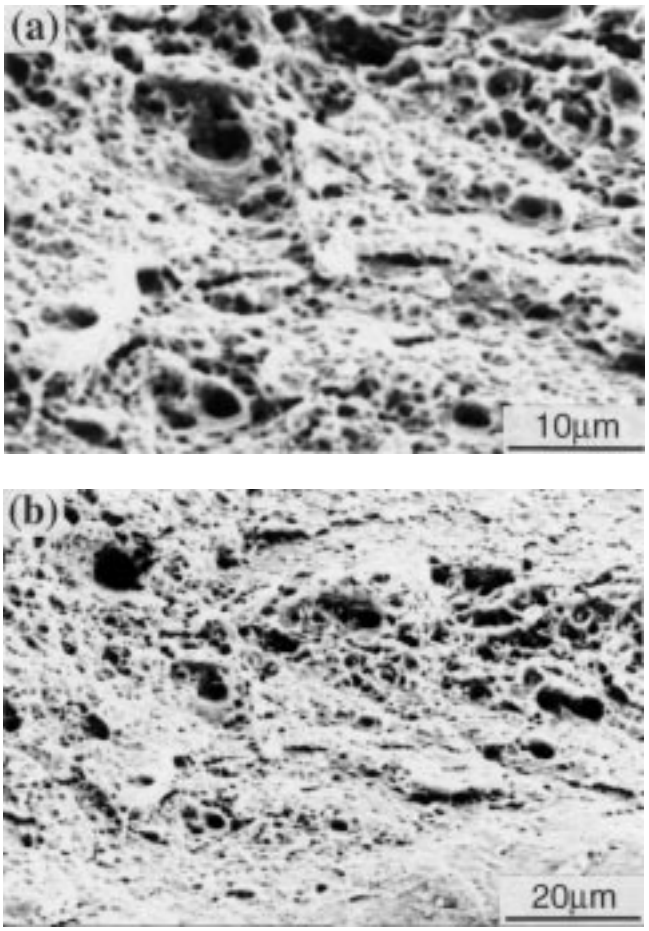

Fig. 4 Fractographs of Zn-22.3Al alloy after tensile testing at room temperature in air. (a) Superplastic specimen. (b) Nonsuperplastic specimen

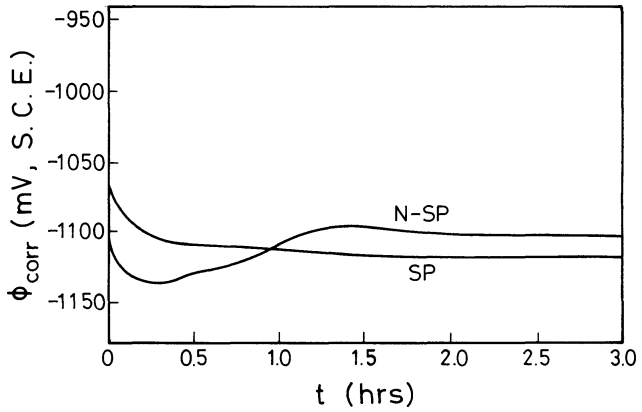

Fig. 5 Variations of corrosion potential (ϕ_{corr}) for superplastic (SP) and nonsuperplastic (N-SP) Zn-22.3Al alloy in 3% NaCl solution

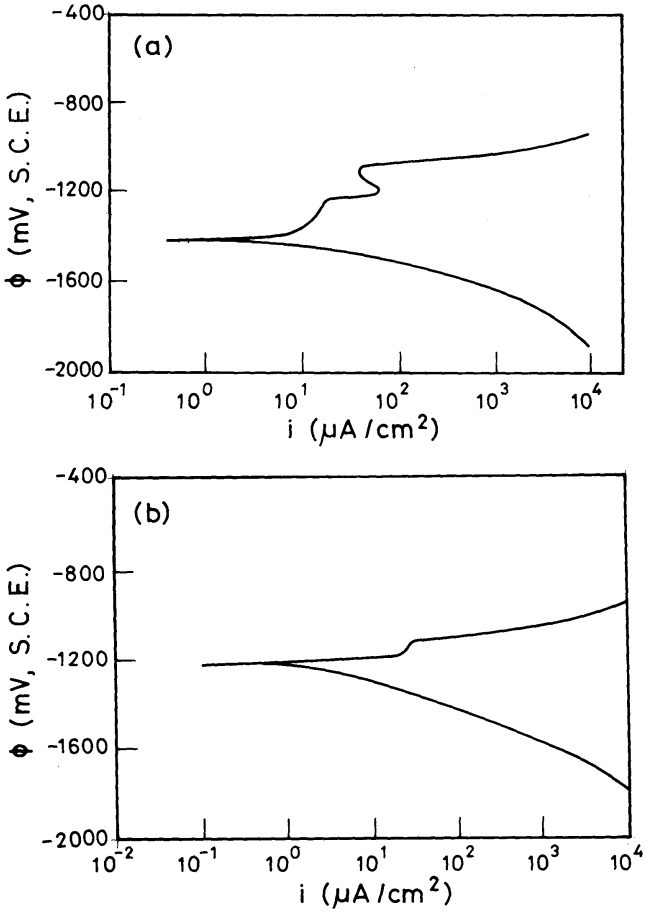

Fig. 6 Dynamic polarization curves of Zn-22.3Al alloy in 3% NaCl solution. (a) Superplastic specimen. (b) Nonsuperplastic specimen

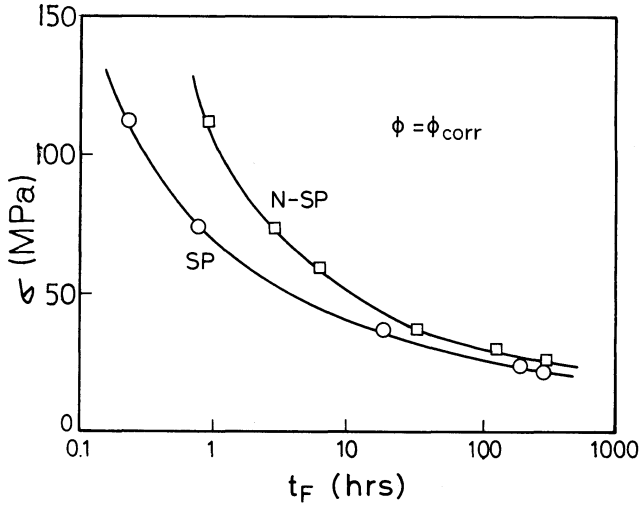

Fig. 7 Fracture times (t_F) of the superplastic (SP) and nonsuperplastic (N-SP) Zn-22.3Al alloy in 3% NaCl solution under open circuit potential and various applied stress (σ)

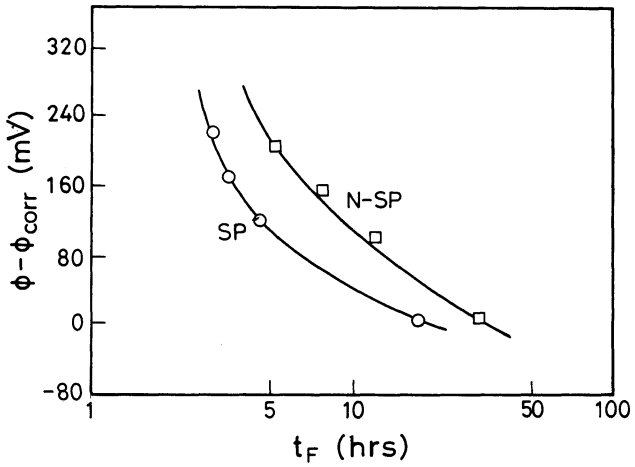

Fig. 8 Fracture times (t_F) of the superplastic (SP) and nonsuperplastic (N-SP) Zn-22.3Al alloy in 3% NaCl solution under an applied stress (σ) of 36.77 MPa (3.75 kg/mm^2) and various anodic potentials ($\phi - \phi_{corr}$)

Table 1 Tensile properties in air and corrosion data in 3% NaCl solution for Zn-22.3Al alloy measured at room temperature

Specimens	Ultimate tensile strength, MPa	Elongation, %	Corrosion potential, mV	Dynamic corrosion potential, mV	Breakdown potential, mV	Corrosion current density, μA/cm^2	Δφ, mV
Superplastic	157	78	–1120	–1403	–1091	16.97	312
Nonsuperplastic	275	17	–1103	–1219	–1127	64.82	92

Δφ is breakdown potential minus dynamic corrosion potential

corrosion current density of the superplastic specimen was much lower than that of the nonsuperplastic specimen. The higher corrosion current density of the nonsuperplastic Zn-22.3Al alloy can also be interpreted by the less uniform distribution of second phases, which resulted in more severe local cell reactions in this alloy. Summarizing from the results of corrosion tests, it is clear that the nonsuperplastic Zn-22.3Al alloy is more sensitive to the environment than the superplastic alloy.

The fracture times of both specimens in 3% NaCl solution at open circuit potential under various applied stress levels are shown in Fig. 7. At higher applied stress, the nonsuperplastic specimen possessed a much longer fracture time than the superplastic specimen, attributable in this case to the dominant effect of higher tensile strength over environmental degradation for the nonsuperplastic Zn-22.3Al alloy. However, as the applied stress decreased, the fracture times of both specimens drew closer. From the corrosion tests, it is shown that a nonsuperplastic Zn-22.3Al alloy has higher environmental sensitivity than a superplastic alloy. At lower applied stress, the anodic dissolution of material caused by the environmental effect balanced with their mechanical properties, which resulted in a closeness of fracture times for both specimens in 3% NaCl solution.

Figure 8 shows the effect of applying various anodic potentials on the fracture times of both specimens in 3% NaCl under a constant stress of 36.77 MPa (3.75 kg/mm^2). It was found that the fracture times of both specimens decreased with an increase in the applied anodic potential. The influence of such an effect of the applied potential was similar for both specimens. However, the fracture time of the nonsuperplastic specimen was longer than that of the superplastic specimen. Since the anodic polarization caused the formation of oxide film on the Zn-22.3Al alloy, the SCC might be attributed to the successive ruptures of the brittle oxide film and ductile Zn-Al matrix. This interpretation is supported by the outer appearances (Fig. 9a and 10a) and fractographs (Fig. 9b and 10b) for both specimens after SCC tests under anodic polarization.

From Fig. 9(a) and 10(a), it can be seen that a series of parallel cracks resulted from the rupture of brittle oxide film appearing on the outer surface of both specimens. Such a phenomenon was more obvious for the superplastic specimen, which can be attributed to the more stable oxide film formed in this specimen under anodic polarization as evidenced by the polarization curves in Fig. 6. After the rupture of the outer oxide film, the crack propagated further into the specimens by tearing apart the Zn-Al matrix and leaving behind a band of dimples on the fractured surface of the specimens. Such a transient-ductile fracture proceeded until a new oxide film formed. The oxide film broke again, and the ductile Zn-Al matrix tore further apart under the applied stress.

The successive processes caused the appearance of a series of parallel strips inserted with bands of dimples as shown on the

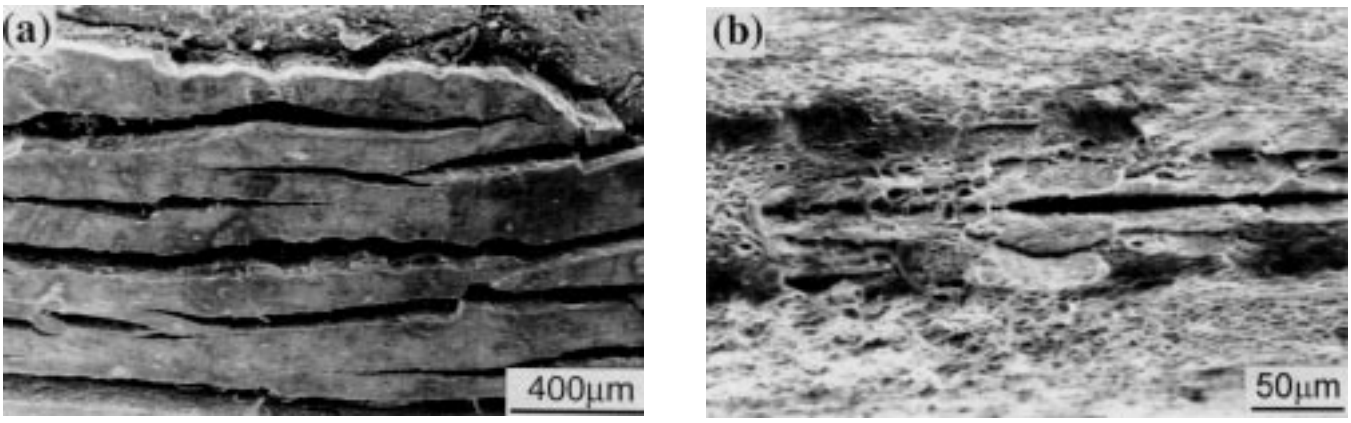

Fig. 9 Observations of superplastic Zn-22.3Al alloy after stress corrosion cracking test in 3% NaCl solution under anodic polarization at an applied stress of 36.77 MPa (3.75 kg/mm^2). (a) Outer appearance. (b) Fractrography

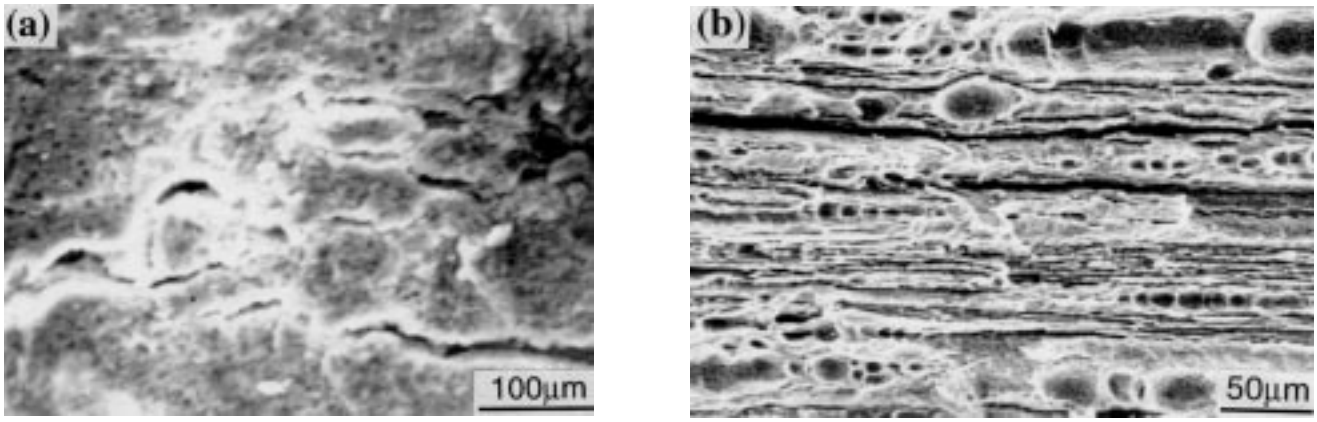

Fig. 10 Observations of nonsuperplastic Zn-22.3Al alloy after stress corrosion cracking test in 3% NaCl solution under anodic polarization at an applied stress of 36.77 MPa (3.75 kg/mm^2). (a) Outer appearance. (b) Fractography

fractographs of Fig. 9(b) and 10(b). Since the superplastic specimen possessed a higher passivation tendency, its formation of oxide film was easier and the rupture process of the oxide film under applied stress dominated over the tearing effect of the Zn-Al matrix. In this case, it is reasonable to note that the appearance of dimple-bands on the fractographs of the superplastic specimen (Fig. 9b) was not as clear as that of the nonsuperplastic specimen (Fig. 10b). The more obvious tearing process accompanying the formation of dimple-bands also resulted in the longer fracture time of nonsuperplastic specimens under anodic polarization, which has been demonstrated in Fig. 8.

4. Conclusions

A Zn-22.3Al alloy after solution treatment at 623 K, quenched in water and kept at room temperature, resulted in a spinodal decomposition, which revealed a microduplex structure. Such specimens possessed superplasticity even at room temperature. Through annealing treatment of the solution-treated Zn-22.3Al alloy at 483 K for 48 h, the specimens transformed into nonsuperplastic lamellar structures. The lamellar second phases coarsened at a certain local position. The uniform distribution of very fine second phases due to the spinodal decomposition caused the superplastic specimens to possess higher corrosion resistance.

The fracture times of both superplastic and nonsuperplastic specimens under lower applied stress at open circuit potential were similar, attributable to the higher environmental sensitivity of the nonsuperplastic Zn-22.3Al alloy balanced with its higher strength for the SCC tests in 3% NaCl solution. Results of SCC under an applied anodic potential can be interpreted by the successive processes of oxide film rupture and Zn-Al matrix tearing evident in a series of parallel strips inserted with a dimple-band on fractographs. The higher passivation tendency of the superplastic specimen caused its formation of oxide film, and the rupture of oxide film dominated the tearing effect of the Zn-Al matrix. Therefore, the fracture time of superplastic specimens remained lower than that of nonsuperplastic specimens under various applied anodic potentials.

References

1 A.A. Bochvar and Z.A. Sviderskaya, Superplasticity in Zinc-Aluminum Alloys, *Izv. Akad, Nauk SSSR, Otdel. Tekh. Nauk.*, Vol 9, 1945, p 821-827
2. A. Ball and M.M Hutchison, *J. Met. Sci.*, Vol 3, 1969, p 1-7
3. T. Oshita and H. Takei, *J. Jpn. Inst. Met.*, Vol 36, 1972, p 1081-1086

4. F.A. Mohamed and T.G. Langdon, *Acta Metall.*, Vol 29, 1981, p 911-920
5. H. Naziri and R. Pearce, *Int. J. Mech. Sci.*, Vol 12, 1970, p 513-520
6. K. Nuttall and R.B. Nicholson, *Philos. Mag. A*, Vol 17 (No. 154), 1968, p 1087-1091
7. R.H. Johnson, C.M. Packer, A.L. Anderson, and O.D. Sherby, *Philos. Mag.*, Vol 18 (No.156), 1968, p 1309-1314
8. H.B. McShane, N. Raghunathan and H.B. Garba, *Powder Metall.*, Vol 33, 1990, p 35-39
9. H.W. Hayden, R.G. Gibsoin, and J. H. Brophy, *Sci. Am.*, Vol 220, 1969, p 28-35
10. L. Gao, *Proc. International Conf. on Superplasticity in Advanced Materials*, S. Hori, M. Tokizane, and N. Furushiro, Ed., The Japan Society for Research on Superplasticity, 1991, p 681-685
11. J. Pilling and N. Ridley, in "Superplasticity in Crystalline Solids," The Institute of Metals, American Publications Center, 1989, p 46-47
12. T.C. Tsai and T.H. Chuang, *Corrosion*, Vol 52, 1996, p 414-416
13. T.C. Tsai and T.H. Chuang, *Metall. Mater. Trans. A*, Vol 27, 1996, p 2617-2627